



**HAL**  
open science

## Ultrastructural and biochemical analyses of hepatitis C virus-associated host cell membranes.

Pauline Ferraris, Emmanuelle Blanchard, Philippe Roingard

► **To cite this version:**

Pauline Ferraris, Emmanuelle Blanchard, Philippe Roingard. Ultrastructural and biochemical analyses of hepatitis C virus-associated host cell membranes.. *Journal of General Virology*, 2010, 91 (Pt 9), pp.2230-7. 10.1099/vir.0.022186-0 . hal-00510829

**HAL Id: hal-00510829**

**<https://hal.science/hal-00510829>**

Submitted on 21 Aug 2010

**HAL** is a multi-disciplinary open access archive for the deposit and dissemination of scientific research documents, whether they are published or not. The documents may come from teaching and research institutions in France or abroad, or from public or private research centers.

L'archive ouverte pluridisciplinaire **HAL**, est destinée au dépôt et à la diffusion de documents scientifiques de niveau recherche, publiés ou non, émanant des établissements d'enseignement et de recherche français ou étrangers, des laboratoires publics ou privés.

**Journal of General Virology 2010 Sep;91(Pt9): 2230-2237**

**PMID : 20484561; Epub 2010 May 19**

## **Ultrastructural and biochemical analyses of hepatitis C virus-associated host cell membranes**

Pauline Ferraris, Emmanuelle Blanchard and Philippe Roingeard\*

INSERM U966, Université François Rabelais and CHRU de Tours, France.

\* Correspondence to: Philippe Roingeard, INSERM U966, Laboratoire de Biologie Cellulaire, Faculté de Médecine de Tours, 10 boulevard Tonnellé, F-37032 Tours Cedex France. Tel: +33 2 47 36 60 71 - Fax: +33 2 47 36 60 90 - E-mail: roingeard@med.univ-tours.fr

### *Summary*

**Like most of other positive-strand RNA viruses, the hepatitis C virus (HCV) induces changes in the host cell membranes, resulting in a membranous web. The nonstructural proteins of the viral replication complex are thought to be associated with these newly synthesized membranes. We studied this phenomenon, using a Huh7.5 cell clone displaying high levels of replication of a subgenomic replicon of the JFH-1 strain. Electron microscopy (EM) of ultrathin sections of these cells revealed the presence of numerous double membrane vesicles (DMVs), resembling those observed for other RNA viruses, such as poliovirus and coronavirus. Some sections had more discrete multivesicular units consisting of circular concentric membranes organized into clusters surrounded by a wrapping membrane. These structures were highly specific to HCV, as they were not detected in naive Huh7.5 cells. Preparations enriched in these structures were separated from other endoplasmic reticulum-derived membranes by cell cytoplasm homogenization and ultracentrifugation on a sucrose gradient. They were found to contain the nonstructural NS3 and NS5A HCV proteins, HCV RNA, and LC3-II, a specific marker of autophagic membranes. By analogy to other viral models, HCV may induce DMVs by activating the autophagy pathway. This could represent a strategy to**

**conceal the viral RNA and help the virus to evade dsRNA-triggered host antiviral responses. More detailed characterization of these virus/cell interactions may facilitate the development of new treatments active against HCV and other RNA viruses dependent on newly synthesized cellular membranes for replication.**

## INTRODUCTION

The formation of a membrane-associated replication complex, consisting of viral proteins, replicating RNA, altered cellular membranes and other host factors, is a hallmark of all positive-strand RNA viruses, including those infecting mammalian, insect or plant cells (Miller & Krijnse-Locker 2008; Mackenzie 2005). Depending on the virus, replication may occur on rearranged convoluted membranes, single- or double-membrane vesicles of various sizes derived from the endoplasmic reticulum (ER), the intermediate compartment between the ER and the Golgi apparatus, the *trans*-Golgi network, mitochondria or even lysosomes (Miller & Krijnse-Locker 2008). These membrane structures induced by positive-strand RNA viruses probably serve as a scaffold for the assembly of viral replication complexes, providing an organization and environment facilitating viral replication (Lyle *et al.*, 2002; Schwartz *et al.*, 2002). Some positive-stranded RNA viruses, including some strains of poliovirus (Jackson *et al.*, 2005), coxsackievirus B3 (Wong *et al.*, 2008) dengue virus (Lee *et al.*, 2008) and mouse hepatitis coronavirus (Prentice *et al.*, 2004) may take over the host autophagy machinery to facilitate their own replication. These positive-stranded RNA viruses trigger autophagosome-like formation without triggering the ultimate degradation of the proteins by the lysosome (Wong *et al.*, 2008). The specific role of autophagic pathway stimulation by these viruses remains unclear (Miller & Krijnse-Locker 2008) but it has been suggested that newly synthesized autophagosomes may provide a physical scaffold for replication complexes, on which viral RNA synthesis may occur (Jackson *et al.*, 2005; Wong *et al.*, 2008; Kirkegaard *et al.*, 2004).

Hepatitis C virus (HCV) is a positive-stranded RNA virus of the Flavivirus family (Penin *et al.*, 2004). The various HCV isolates have been grouped into six major genotypes and many more subtypes on the basis of their genetic similarities. HCV is a major cause of chronic hepatitis, liver cirrhosis and hepatocellular carcinoma worldwide (Shepard *et al.*, 2005). Treatment is currently limited, so intensive efforts are being made to identify antiviral drugs active against different steps of the HCV infectious cycle (Pawlotsky *et al.*, 2007). The HCV

genome encodes a large polyprotein precursor of about 3000 amino acids, which is co- and posttranslationally processed by cellular and viral proteases to yield the mature structural proteins — core and envelope proteins (E1 and E2) — and the nonstructural proteins p7, NS2, NS3, NS4A, NS4B, NS5A, and NS5B (Penin *et al.*, 2004). Proteins NS3 to NS5B form a replicase that has been shown to be sufficient for autonomous HCV RNA replication in a subgenomic replicon model (Lohmann *et al.*, 1999; Blight *et al.*, 2000). A specific change in membrane structure, the formation of a membranous web, has been identified by electron microscopy (EM) as the principal site of viral RNA replication in Huh7 hepatoma cells harboring a subgenomic replicon from a 1b genotype virus (Gosert *et al.*, 2003). This membranous web consisted of vesicles, 80 to 100 nm in diameter, embedded in a membrane matrix resembling the discrete inclusions previously identified on EM of liver samples from HCV-infected chimpanzees (Egger *et al.*, 2002). EM investigations (Egger *et al.*, 2002; Gosert *et al.*, 2003) and biochemical analyses of purified membranes associated with the HCV replication complexes (Miyanari *et al.*, 2003; El-Hage *et al.*, 2003; Huang *et al.*, 2007) have suggested that the HCV-induced membranous web is derived from ER membranes, although it may also contain early endosome proteins, including Rab5 (Stone *et al.*, 2007). Independent reports have recently suggested that the autophagy machinery is required for the HCV life cycle (Ait-Goughoulte *et al.*, 2008; Sir *et al.*, 2008; Dreux *et al.*, 2009; Tanida *et al.*, 2009). This has been shown to be the case in cells harboring a subgenomic replicon or supporting the complete viral life cycle, and for different genotypes. Like poliovirus and coxsackievirus B3, HCV induces the accumulation of autophagosomes, but does not increase the rate of autophagic protein degradation. However, these studies provided conflicting results concerning the stage of the HCV life cycle requiring the autophagy machinery, and it remains unclear if there is a connection between the HCV membranous web and these autophagosomes. The membranous web is not frequently encountered on EM of sections of cells harboring a subgenomic HCV 1b replicon (Gosert *et al.*, 2003; P. Ferraris & P. Roingard, personal observations) and this structure remains poorly understood. The identification of an HCV isolate of 2a genotype (JFH-1 strain) capable of high levels of replication in the Huh7 cell line without the need for mutations conferring adaptation to cell culture has finally made it possible to establish an *in vitro* cell culture system for HCV (Wakita *et al.*, 2005; Lindenbach *et al.*, 2005; Zhong *et al.*, 2005). However, this particular strain induces the formation of highly complex membrane structures in infected cells (Miller & Krijnse-Locker 2008; Welsch *et al.*, 2009), and the detailed analysis of these structures is extremely difficult (Welsh *et al.*, 2009). Biochemical analyses of a purified membranous web

combined with EM and negative staining analysis have been very informative for models such as poliovirus (Egger *et al.*, 1996), but no studies of this type have been reported for HCV. We therefore made use of a similar approach and the strong replication of the HCV JFH-1 isolate to investigate the cellular membranes associated with HCV RNA and proteins in the context of a subgenomic replicon.

## RESULTS

### EM analysis of the intracellular changes associated with JFH-1 strain replication

Huh7.5-C5 cells harboring the JFH-1 subgenomic replicon displayed significant and highly specific ultrastructural modifications on EM (Fig. 1 A, B and C), as shown by comparisons with uninfected Huh7.5 control cells (Fig. 1D). The cytoplasm of the Huh7.5-C5 cells contained numerous 200 to 500 nm-wide double membrane vesicles (DMVs; Fig. 1A and 1B). These vesicles were initially thought to consist of a single very thick, electron-dense membrane, but careful examination at high magnification revealed the presence of a double membrane in some areas, suggesting a tight association of the two membranes in these vesicles (inset in Fig. 1A and 1B), as reported for similar structures in cells infected with coronavirus (Snijder *et al.*, 2006). We estimated the frequency of these DMVs, by determining the number of these vesicles in 60 consecutive cell sections, for both Huh7.5-C5 and Huh7.5 cells. The mean number of DMVs was 0.4 per  $\mu\text{m}^2$  for Huh7.5-C5 cells and 0.01 per  $\mu\text{m}^2$  for Huh7.5 cells (or 37 DMVs per cell section for Huh7.5-C5 cells versus 1 for Huh7.5 cells).

In some cell sections, we also found highly organized vesicular structures up to 800 nm in diameter (Fig. 1C). These larger vesicles were delimited by a single membrane, and contained smaller circular vesicular structures 150 to 200 nm in diameter. Each of these smaller units seemed to contain a dense core surrounded by several concentric membranes (Fig. 1C).

### **Isolation of host cell membranes associated with the HCV RNA and proteins on a sucrose gradient**

All fractions with a density between 1.02 and 1.27 g/cm<sup>3</sup> were positive for the ER marker calreticulin, in both the Huh7.5-C5 and Huh7.5 cell lines (Fig. 2A). Only fractions with a density of 1.18 to 1.27 g/cm<sup>3</sup> for Huh7.5-C5 cells displayed strong staining for the LC3-II protein and weaker staining for the LC3-I protein. The three LC3-II-positive fractions of the Huh7.5-C5 cell line also tested positive for the NS3 and NS5A proteins and were the fractions containing the largest amounts of HCV RNA (Fig. 2A). Thus, the membranes associated with HCV RNA and proteins contained ER markers, but could be separated from other ER membranes. These ER-derived membranes specifically associated with HCV RNA and proteins contained markers of the autophagy machinery, whereas the equivalent fractions from the control cells tested negative for LC3-I and LC3-II (Fig. 2A).

### **EM analysis of the purified membranes associated with HCV RNA and proteins**

We investigated the ultrastructure of the membranes associated with HCV RNA and proteins and specifically induced by HCV replication, by EM with negative staining, based on direct comparisons of the membranous structures in the selected fractions of Huh7.5-C5 cells and the equivalent fractions of Huh7.5 control cells (Fig. 2B). The membranes associated with HCV were connected to nonspecific, probably ER-derived membranes also present in control cells (see the smooth membranes delimited by white arrowheads in Fig. 2B-a and the same structures in Fig. 2B-b). However, additional highly specific structures were observed exclusively in the purified Huh7.5-C5 membranes. These specific structures included numerous 200 to 500 nm-wide vesicles with a very thick membrane (black arrows in Fig. 2B-a), connected to nonspecific ER membranes. These structures were probably the DMVs encountered in cell sections shown in Fig. 1A and 1B. As expected, their membranes appeared wide and clear on negative staining, as the uranyl acetate could not penetrate between the tightly associated membranes. The other specific structures were small (150 to 200 nm wide) circular units consisting of concentric membranes (black arrows in Fig. 2B-c). These small units, which seemed to be surrounded by wrapping membranes, were less frequently encountered and probably corresponded to the structures observed in the cell sections shown in Fig. 1C.

### **Immuno-EM analysis of the DMVs in Huh7.5-C5 cells prepared by cryosubstitution**

We confirmed the specificity of our observations, by carrying out immunogold labeling to localize the viral dsRNA, NS5A and LC3 in Huh7.5-C5 cells. Anti-LC3 antibodies gave a strong background on immuno-EM, so we transfected Huh7.5-C5 cells with pEGFP-LC3 and then detected LC3 with anti-GFP antibodies. The viral RNA was detected with the anti-dsRNA J2 monoclonal antibody, which has been shown to detect the HCV dsRNA in cells replicating HCV (Targett-Adams *et al.*, 2008). The fixation and embedding procedure for this specific immunostaining method resulted in the cell structures, including the DMVs in particular, being less well preserved than in cells embedded in epon resin according to standard EM methods (Fig. 3). A faint but specific immuno-gold signal for dsRNA was detected within the DMVs (Fig. 3A). By counting and analyzing the subcellular localization of the gold particles in 10 consecutive cell sections, we determined that 68% of the gold particles were localized in the DMVs, and less than 13% of gold particles in control compartments (mitochondria and nucleus). Immunogold labeling for NS5A was observed at the inner membrane of the DMVs (Fig. 3B) and within some of the circular units consisting of concentric membranes (Fig. 3C). In this case, 65% of the gold particles were localized in the DMVs, and less than 15% of gold particles in mitochondria or nucleus. Finally, immuno-EM with the anti-GFP antibody strongly decorated the membranes surrounding the DMVs (Fig. 3D). All these observations were specific to Huh7.5-C5 cells, as no immunogold labeling was detected in the Huh7.5 control cells (data not shown).

## **DISCUSSION**

The induction of host cell membrane rearrangements, probably creating a scaffold for the assembly of viral replication complexes, has been described in almost all groups of positive-strand RNA viruses, but the architecture and origin of the resulting membrane structures differ between viral groups (Miller & Krijnse-Locker 2008). For HCV, it has been suggested that the induced membrane alterations are particularly heterogeneous, with irregular assemblies of membranous vesicles (Miller & Krijnse-Locker 2008 ; Welsch *et al.*, 2009). This situation makes it much more difficult to analyze these complex structures for HCV than for other members of the Flavivirus family. We demonstrate here that the replication of a subgenomic replicon of the HCV JFH-1 strain induces numerous 200 to 500 nm-wide double-

membrane vesicles (DMVs) (Fig. 1A, 1B and 1C), similar to those described for poliovirus (Schlegel *et al.*, 1996), the severe acute respiratory syndrome (SARS) coronavirus (Snijder *et al.*, 2006) and coxsackievirus B3 (Wong *et al.*, 2008). We also identified some DMVs on EM sections of cells harboring a subgenomic HCV 1b replicon, but in much smaller numbers. By contrast, DMVs were also frequently observed in other clones of Huh7.5 cells containing a JFH-1 subgenomic replicon (data not shown). In the SARS virus model, these virus-induced, ER-derived vesicles seem to have a thick, dense membrane, but careful EM examination has revealed the presence of double membrane (Snijder *et al.*, 2006), a feature also found in the HCV-induced vesicles. These DMVs were initially thought to carry the SARS virus replication complexes (Snijder *et al.*, 2006), but more recent studies have clearly demonstrated that DMVs contain some nonstructural proteins, but mostly double-stranded RNA, and that their contents do not appear to be connected to the cytoplasm (Knoops *et al.*, 2008). These findings led to suggestions that DMVs may help to conceal the viral RNA, enabling the virus to evade the dsRNA-triggered antiviral responses of the host, such as those mediated by the double-stranded RNA-dependent protein kinase (Knoops *et al.*, 2008). The same SARS model demonstrated that viral replication occurs preferentially in circular structures known as convoluted membranes (Knoops *et al.*, 2008), which may be precursors of DMVs. These structures were found to be identical to the “reticular inclusions” first observed in cells infected with mouse hepatitis coronavirus (MHV) more than 40 years ago (David-Ferreira & Manaker 1965), and subsequently referred to as “clusters of tubular cisternal elements” (Krijnse-Locker *et al.*, 1994). The small circular units observed in HCV RNA-replicating cells in our study (Fig. 1C) also resembled these previously described structures. It remains unclear whether the similar ultrastructural changes observed in cells replicating the HCV and SARS viruses reflect a similar intracellular organization for these viruses from two different families.

However, we were able to demonstrate that these specific HCV-induced structures (i.e. the DMVs and the circular units consisting of a dense core with concentric membranes and surrounded by a wrapping membrane) were frequently present in semi-purified ER-derived membranes containing the HCV RNA and proteins. These structures were closely connected to ER membranes and highly specific for HCV, as they were never observed with material purified from the control cells. Unfortunately, the immunogold labeling of this material for negative-staining EM was unsuccessful (data not shown), despite the use of methods successful in other studies (Chapel *et al.*, 2007). The HCV nonstructural proteins and dsRNA



may not have been accessible to the antibodies in this case, as they are thought to be associated with the inner membrane of the HCV-induced vesicles (Miller & Krijnse-Locker 2008; Quinkert *et al.*, 2005). Nevertheless, immuno-EM analysis of ultrathin sections of cells prepared by cryosubstitution suggested that NS5A was present at the inner membrane of the HCV-induced DMVs, whereas the lumen of these DMVs appeared to contain some viral RNA. In addition, NS5A was observed within the circular units with concentric membranes. These results suggest that there are similarities in the intracellular organization of HCV and SARS viruses, although this assertion requires confirmation in further studies. Our observation is consistent with biochemical and ultrastructural analyses of the replication complexes of various viruses of the Flaviridae family. In studies using detergents, trypsin and nucleases, it has been suggested that the replication complexes of the West Nile virus, the Japanese encephalitis virus and the dengue virus are probably enclosed in a double-membrane compartment (Uchil & Satchidanandam 2003). It has also been suggested, on the basis of EM, that the replication complexes of the dengue virus (Mackenzie *et al.*, 1996) and the Kunjin virus — the Australian strain of the West Nile virus — (Westaway *et al.*, 1997) are found in small vesicles surrounded by an outer limiting membrane holding them together in clusters.

The viral components of many viruses capable of subverting the autophagy machinery for their own replication, including poliovirus (Jackson *et al.*, 2005; Taylor & Kirkegaard 2007), mouse hepatitis coronavirus (Prentice *et al.*, 2004), coxsackievirus B3 (Wong *et al.*, 2008) and dengue virus (Lee *et al.*, 2008), colocalize with the autophagy marker LC3, suggesting that the replication complexes of these viruses may assemble on autophagic vesicles. In the poliovirus model, it has been suggested that the membrane-associated viral protein 2BC initially recruits the cytoplasmic protein LC3-I. LC3-I would then be converted, by the autophagic machinery, into the lipidated species LC3-II, which could remain firmly associated with the autophagosome membrane (Taylor & Kirkegaard 2009). It is thought that these virus-induced DMVs are similar to the autophagosome used for normal cellular autophagy, but smaller (Taylor & Kirkegaard 2009). We provide the first demonstration, by western blotting, that fractions enriched in HCV-induced DMVs contain LC3-II. ER-derived membranes purified from control cells were, as expected, free of LC3, as this protein is cytoplasmic in cells in which the autophagic pathway is not induced. Moreover, our immuno-EM experiments on cell sections demonstrated that the membranes of the HCV-induced DMVs were strongly positive for LC3, providing additional support for the hypothesis that these DMVs have characteristics typical of autophagosomes. The weak colocalization of

HCV nonstructural protein with LC3 reported elsewhere (Ait-Goughoulte *et al.*, 2008; Sir *et al.*, 2008; Dreux *et al.*, 2009; Tanida *et al.*, 2009) may be accounted for by HCV-induced DMVs containing principally viral RNA, as reported for the SARS virus (Knoops *et al.*, 2008). The presence of the HCV nonstructural proteins in our LC3-positive fractions may be due to ER-derived membranes including the circular units with concentric membranes containing these nonstructural proteins being distinct, but interconnected with the DMVs, leading to cosedimentation during subcellular fractionation with gentle conditions.

HCV has been reported to subvert, preempt and antagonize the innate immune system at multiple levels (Rehermann 2009). The concealment of its replicated RNA from the host cell antiviral defense system in DMVs may constitute an additional mechanism of escape from the innate immune response. Alternatively, autophagic membranes in cells replicating HCV RNA may be induced by the innate immune response itself. Autophagy is known to be principally a functional pathway in the immune response to several viruses, intracellular bacteria or parasites (Kirkegaard *et al.*, 2004). This response may be cell-dependent, and the large number of DMVs in Huh7.5 cells harboring the HCV JFH-1 subgenomic replicon may result from the high levels of replication of this HCV strain, intrinsic properties of this particular clone of the Huh7 cell line, or both. Further analysis of the structure, interactions and function of the membranes associated with HCV RNA and proteins are required to test this hypothesis. Improvements in our understanding of HCV/host cell interactions may ultimately lead to more effective antiviral treatments and a better prognosis for chronic HCV carriers. Such improvements in our understanding might also lead to the development of new treatments for infections with other RNA viruses dependent on newly formed cellular membranes for replication.

## METHODS

**Cell culture.** The Huh7.5 cell line (gift from Dr Rice, Rockefeller University, New York, NY) is a clone of the human hepatoma cell line Huh7, obtained by curing stably selected replicon-containing cells with interferon, and thus supporting efficient HCV replication (Blight *et al.*, 2002). This cell line was grown in Dulbecco's modified Eagle's medium (DMEM, Invitrogen) supplemented with 10% fetal calf serum, and 100 µg/ml penicillin and streptomycin (Invitrogen). Huh7.5 cells were transfected with *in vitro* transcripts of the linearized pSGR-JFH1 plasmid (gift from Dr Wakita, National Institute of Infectious

Diseases, Tokyo, Japan), which contains the nucleotide sequence of the JFH-1 strain subgenomic replicon and a neomycin resistance gene, as previously described (Kato *et al.*, 2003). Cells were cultured in G418-containing medium to select several resistant clones, whereas cells transfected with *in vitro* transcripts of the replication-defective GND mutant (gift from Dr Wakita) were used as a control (Kato *et al.*, 2003). Several resistant clones were amplified and their intracellular viral RNA content was determined with the Abbott m2000<sub>sp</sub>-m2000<sub>rt</sub> real-time PCR assay (Chevaliez *et al.*, 2009), according to the protocol provided by the manufacturer. For our main subsequent investigations, we selected the clone with the largest amount of intracellular RNA, Huh7.5-C5, which contained more than 1500 IU/HCV RNA per cell at initial subculture. For some experiments, this clone and the control cells were further transfected with pEGFP-LC3 (Kabeya *et al.*, 2000; gift from Dr Noboru Mizushima, Medical and Dental University, Tokyo, Japan), with Fugene, according to the standard protocols provided by the manufacturer (Roche).

**Isolation of host cell membranes associated with HCV RNA and proteins.** We established a protocol adapted from various reports on the purification of host cell membranes associated with the replication complexes of the Kunjin virus (Chu & Westaway 1992; Chu *et al.*, 1992) and poliovirus (Egger *et al.*, 1996). Huh7.5-C5 and Huh7.5 (control) cells were amplified to obtain 100 million cells, which were resuspended in 10 mM sodium acetate, 10 mM Tris-HCl pH 8.0, 1.5 mM MgCl<sub>2</sub>, 1 mM phenylmethylsulfonyl fluoride, 2 µg/ml aprotinin and 2 µg/ml leupeptin (TNMg buffer), and gently homogenized with a Dounce homogenizer. After centrifugation at 500 x g for 10 minutes at 4°C, the cytoplasmic extracts were layered onto a double sucrose cushion of 30% and 40% (w/v in TNMg buffer), and centrifuged again at 40,000 rpm (SW 41 rotor, Beckman) for 2 h at 4°C. The pellets were resuspended carefully in TNMg buffer and disrupted by several slow passages through a 21-gauge hypodermic needle. These preparations were then layered onto a discontinuous sucrose gradient (2.0 ml 80%, 2.0 ml 70%, 2.5 ml 60%, 2 ml 40%, 2 ml 30%; w/v in TNMg buffer) and centrifuged at 40,000 rpm (SW41 rotor, Beckman) for 2 h at 4°C. The densities of the 11 fractions collected with a peristaltic pump were determined by refractometry (AOC, American Optical Corporation). Fractions were then analyzed for the presence of HCV RNA and proteins. Viral RNA was quantified with the Abbott m2000<sub>sp</sub>-m2000<sub>rt</sub> real-time PCR assay. The nonstructural viral proteins NS3 and NS5A were detected by western blotting. Briefly, each fraction collected was separated by SDS-PAGE in 12 % polyacrylamide gels and the resulting bands were transferred to a nitrocellulose membrane. The membrane was blocked by incubation in 0.1 %

(vol/vol) NP-40 in TBS supplemented with 5 % (wt/vol) skimmed milk powder (TBS-N). Membranes were incubated with polyclonal sheep antibodies against NS5A and NS3 (provided by Dr Harris, University of Leeds, UK) diluted 1:2000 in TBS-N, washed and incubated with a horseradish peroxidase-conjugated anti-sheep antibody diluted 1:10000 in TBS-N. Antibody binding was detected by enhanced chemiluminescence (ECL, ThermoFisher). These fractions were further characterized by western blotting for the presence of ER and autophagic membrane markers: calreticulin and LC3, respectively. Blots were incubated with a monoclonal anti-calreticulin (BD Biosciences) and a rabbit polyclonal anti-LC3 (Abcam) antibody as described above, and antibody binding was detected with an appropriate horseradish peroxidase-conjugated secondary antibody.

**Electron microscopy.** For standard ultrastructural analysis by EM, cells were treated as previously described (Hourieux *et al.*, 2007). Briefly, cells were fixed by incubation for 48 hours in 4 % paraformaldehyde and 1 % glutaraldehyde in 0.1 M phosphate buffer pH 7.2, washed in PBS, postfixed by incubation for 1 hour with 1 % osmium tetroxide and dehydrated in a graded series of ethanol solutions. Cell pellets were embedded in Epon resin (Sigma), which was allowed to polymerize for 48 hours at 60°C. Ultrathin sections were cut, stained with 5 % uranyl acetate and 5 % lead citrate, and deposited on EM grids coated with collodion membrane, for examination under a Jeol 1230 transmission electron microscope (TEM). For ultrastructural analysis of the fractions collected from the sucrose gradient, 10  $\mu$ l of each fraction was deposited on EM carbon-coated grids, negatively stained with 1 % uranyl acetate, and analyzed under the TEM.

**Immuno-EM.** Huh7.5-C5 cells or Huh7.5 control cells transfected with pGFP-LC3 were fixed 48 h after transfection, by incubation in 4% paraformaldehyde in 0.1 M phosphate buffer (pH 7.2) for 20 h. The cells were collected by centrifugation and the cell pellet was then dehydrated in a graded series of ethanol solutions at  $-20^{\circ}\text{C}$ , using an automatic freezing substitution system (AFS, Leica), and embedded in London Resin Gold (LR Gold, Electron Microscopy Science). The resin was allowed to polymerize at  $-25^{\circ}\text{C}$ , under UV light, for 72 h. Ultrathin sections were cut and blocked by incubation with 3% fraction V bovine serum albumin (BSA, Sigma) in PBS. They were then incubated with the anti-dsRNA J2 monoclonal antibody (Scicons), the polyclonal anti-NS5A antibody described above, or with a polyclonal anti-GFP rabbit antibody (Abcam) diluted 1:50 in PBS supplemented with 1% BSA. Sections were then washed and incubated with an appropriate 15 nm gold particle-

conjugated secondary antibody (British Biocell International) diluted 1:50 in PBS supplemented with 1% BSA. Ultrathin sections were cut, stained with 5 % uranyl acetate, 5 % lead citrate, placed on EM grids coated with collodion and observed as described above.

## ACKNOWLEDGMENTS

This work was supported by a grant from ANRS (*Association Nationale pour la Recherche sur le Sida et les hépatites virales*), France. P.F. was supported by a PhD fellowship from the ANRS. We thank Dr Mark Harris, Dr Noboru Mizushima, Dr Charles M Rice and Dr Takaji Wakita for providing us with useful biological materials and reagents. We thank Sylvie Trassard, Fabienne Arcanger and Monique Lemesle for technical assistance with EM sections, and Pierre-Yves Sizaret for assistance with negative-staining EM. We thank Catherine Gaudy and Alain Goudeau for HCV RNA quantifications, as well as Christophe Hourieux and Faraj Terro for helpful discussions on this work. Our data were obtained with the assistance of the RIO Electron Microscopy Facility of François Rabelais University.

## REFERENCES

- Ait-Goughoulte, M., Kanda, T., Meyer, K., Ryerse, J.S., Ray, R.B. & Ray R. (2008).** Hepatitis C virus genotype 1a growth and induction of autophagy. *J Virol* **82**, 2241-2249.
- Blight, K.J., Kolykhalov, A.A., & Rice C.M. (2000).** Efficient initiation of HCV RNA replication in cell culture. *Science* **290**, 1972-1974.
- Blight, K.J., McKeating, J.A. & Rice, C.M. (2002).** Highly permissive cell lines for subgenomic and genomic hepatitis C virus RNA replication. *J Virol* **76**, 13001-13014.
- Chapel, C., Garcia, C., Bartosch, B., Roingeard, P., Zitzmann, N., Cosset, F.L., Dubuisson, J., Dwek, R.A., Trépo, C., Zoulim, F. & Durantel, D. (2007).** Reduction of the infectivity of hepatitis C virus pseudoparticles by incorporation of misfolded glycoproteins induced by glucosidase inhibitors. *J Gen Virol* **88**, 1133-43.
- Chevaliez, S., Bouvier-Alias, M. & Pawlotsky, J.M. (2009).** Performance of the Abbott real-time PCR assay using m2000sp and m2000rt for hepatitis C virus RNA quantification. *J Clin Microbiol* **47**, 1726-1732.
- Chu, P.W. & Westaway, E.G. (1992).** Molecular and ultrastructural analysis of heavy membrane fractions associated with the replication of Kunjin virus RNA. *Arch Virol* **125**, 177-191.

- Chu, P.W., Westaway, E.G. & Coia, G. (1992).** Comparison of centrifugation methods for molecular and morphological analysis of membranes associated with RNA replication of the flavivirus Kunjin. *J Virol Methods* **37**, 219-234.
- David-Ferreira, J.F. & Manaker, R.A. (1965).** An electron microscope study of the development of a mouse hepatitis virus in tissue culture cells. *J Cell Biol* **24**, 57-78.
- Dreux, M., Gastaminza, P., Wieland, S.F. & Chisari, F.V. (2009).** The autophagy machinery is required to initiate hepatitis C virus replication. *Proc Natl Acad Sci USA* **106**, 14046-14051.
- Egger, D., Pasamontes, L., Bolten, R., Boyko, V. & Bienz, K. (1996).** Reversible dissociation of the poliovirus replication complex: functions and interactions of its components in viral RNA synthesis. *J Virol* **70**, 8675-8683.
- Egger, D., Wölk, B., Gosert, R., Bianchi, L., Blum, H.E., Moradpour, D. & Bienz, K. (2002).** Expression of hepatitis C virus proteins induces distinct membrane alterations including a candidate viral replication complex. *J Virol* **76**, 5974-5984.
- El-Hage, N. & Luo, G. (2003).** Replication of hepatitis C virus RNA occurs in a membrane-bound replication complex containing nonstructural viral proteins and RNA. *J Gen Virol* **84**, 2761-2769.
- Gosert, R., Egger, D., Lohmann, V., Bartenschlager, R., Blum, B.H., Bienz, K. & Moradpour, D. (2003).** Identification of the hepatitis C virus RNA replication complex in Huh-7 cells harboring subgenomic replicons. *J Virol* **77**, 5487-5492.
- Hourioux, C., Patient, R., Morin, A., Blanchard, E., Moreau, A., Trassard, S., Giraudeau, B. & Roingard, P. (2007).** The genotype 3-specific hepatitis C virus core protein residue phenylalanine 164 increases steatosis in an *in vitro* cellular model. *Gut* **56**, 1302-1308.
- Huang, H., Sun, F., Owen, D.M., Li, W., Chen, Y., Gale Jr, M. & Ye, J. (2007).** Hepatitis C virus production by human hepatocytes dependent on assembly and secretion of very low-density lipoproteins. *Proc Natl Acad Sci USA* **104**, 5848-5853.
- Jackson, W.T., Giddings, Jr T.H., Taylor, M.P., Mulinyawe, S., Rabinovitch, M., Kopito, R.R. & Kirkegaard, K. (2005).** Subversion of cellular autophagosomal machinery by RNA viruses. *PLoS Biol* **3**, e156.
- Kabeja, Y., Mizushima, N., Ueno, T., Yamamoto, A., Kirisako, T., Noda, T., Kominami, E., Ohsumi, Y., Yoshimori, T. (2000).** LC3, a mammalian homologue of yeast Apg8p, is localized in autophagosome membranes after processing. *EMBO J* **19**, 5720-5728.

- Kato, T., Date, T., Miyamoto, M., Furusaka, A., Tokushige, K., Mizokami, M. & Wakita, T. (2003).** Efficient replication of the genotype 2a hepatitis C virus subgenomic replicon. *Gastroenterology* **125**, 1808-1817.
- Kirkegaard, K., Taylor, M.P., & Jackson, W.T. (2004)** Cellular autophagy: surrender, avoidance and subversion by microorganisms. *Nat Rev Microbiol* **2**, 301-314.
- Knoops, K., Kikkert, M., Worm, S.H., Zevenhoven-Dobbe, J.C., van der Meer, Y., Koster, A.J., Mommaas, A.M. & Snijder, E.J. (2008).** SARS-coronavirus replication is supported by a reticulovesicular network of modified endoplasmic reticulum. *PLoS Biol* **6**, e226.
- Krijnse-Locker, J., Ericsson, M., Rottier, P.J. & Griffiths, G. (1994).** Characterization of the budding compartment of mouse hepatitis virus: evidence that transport from the RER to the Golgi complex requires only one vesicular transport step. *J Cell Biol* **124**, 55-70.
- Lee, Y.R., Lei, H.Y., Liu, M.T., Wang, J.R., Chen, S.H., Jiang-Shieh, Y.F., Lin, Y.S., Yeh, T.M., Liu, C.C. & Liu, H.S. (2008).** Autophagic machinery activated by dengue virus enhances virus replication. *Virology* **374**, 240-248.
- Lindenbach, B.D., Evans, M.J., Syder, A.J., Wölk, B., Tellinghuisen, T.L., Liu, C.C., Maruyama, T., Hynes, R.O., Burton, D.R., McKeating, J.A. & Rice, C.M. (2005).** Complete replication of hepatitis C virus in cell culture. *Science* **309**, 623-626.
- Lohmann, V., Körner, F., Koch, J., Herian, U., Theilmann, L., & Bartenschlager R. (1999).** Replication of subgenomic hepatitis C virus RNAs in a hepatoma cell line. *Science* **285**, 110-113.
- Lyle, J.M., Clewell, A., Richmond, K., Richards, O.C., Hope, D.A., Schultz, S.C. and Kirkegaard, K. (2002).** Similar structural basis for membrane localization and protein priming by an RNA-dependent RNA polymerase. *J Biol Chem* **277**, 16324-16331.
- Mackenzie, J.M. (2005).** Wrapping things up about virus RNA replication. *Traffic* **6**, 967-977.
- Mackenzie, J.M, Jones, M.K. & Young, PR. (1996).** Immunolocalization of the dengue virus nonstructural glycoprotein NS1 suggests a role in viral RNA replication. *Virology* **220**, 232-240.
- Miller, S. & Krijnse-Locker, J. (2008).** Modification of intracellular membrane structures for virus replication. *Nat Rev Microbiol* **6**, 363-374.
- Miyanari, Y., Hijikata, M., Yamaji, M., Hosaka, M., Takahashi, H. & Shimotohno K. (2003).** Hepatitis C virus non-structural proteins in the probable membranous compartment function in viral genome replication. *J Biol Chem* **278**, 50301-50308.

- Pawlotsky, J.M., Chevaliez, S. & McHutchison, J.G. (2007)** The hepatitis C virus life cycle as a target for new antiviral therapies. *Gastroenterology* **132**, 1979-1998.
- Penin, F., Dubuisson, J., Rey, F.A., Moradpour, D. & Pawlotsky, J.M. (2004).** Structural biology of hepatitis C virus. *Hepatology* **39**, 5-19.
- Prentice, E., Jerome, W.G., Yoshimori, T., Mizushima, N., & Denison, M.R. (2004).** Coronavirus replication complex formation utilizes components of cellular autophagy. *J Biol Chem* **279**, 10136-10141.
- Quinkert, D., Bartenschlager, R. & Lohmann, V. (2005).** Quantitative analysis of the hepatitis C virus replication complex. *J Virol* **79**, 13594-13605.
- Rehermann, B. (2009).** Hepatitis C virus versus innate and adaptive immune responses: a tale of coevolution and coexistence. *J Clin Invest* **119**, 1745-1754.
- Schlegel, A., Giddings Jr, T.H., Ladinsky, M.S. & Kirkegaard, K. (1996).** Cellular origin and ultrastructure of membranes induced during poliovirus infection. *J Virol* **10**, 6576-6588.
- Schwartz, M., Chen, J., Janda, M., Sullivan, M., den Boon, J. & Ahlquist P. (2002).** A positive-strand RNA virus replication complex parallels form and function of retrovirus capsids. *Mol Cell* **9**, 505-514.
- Shepard CW, Finelli L, Alter MJ (2005).** Global epidemiology of hepatitis C virus infection. *Lancet Infect Dis* **5**, 558-567.
- Sir, D., Chen, W.L., Choi, J., Wakita, T., Yen, T.S. & Ou, J.H. (2008).** Induction of incomplete autophagic response by hepatitis C virus via the unfolded protein response. *Hepatology* **48**, 1054-1061.
- Snijder, E.J., van der Meer, Y., Zevenhoven-Dobbe, J., Onderwater, J.J., van der Meulen, J., Koerten, H.K. & Mommaas, A.M. (2006).** Ultrastructure and origin of membrane vesicles associated with the severe acute respiratory syndrome coronavirus replication complex. *J Virol* **80**, 5927-5940.
- Stone, M., Jia, S., Heo, W.D., Meyer, T. & Konan, K.V. (2007).** Participation of rab5, an early endosome protein, in hepatitis C virus RNA replication machinery. *J Virol* **81**, 4551-4563.
- Tanida, I., Fukasawa, M., Ueno, T., Kominami, E., Wakita, T. & Hanada, K. (2009).** Knockdown of autophagy-related gene decreases the production of infectious hepatitis C virus particles. *Autophagy* **5**, 937-945.
- Targett-Adams P, Boulant S, McLauchlan J. (2008).** Visualization of double-stranded RNA in cells supporting hepatitis C virus RNA replication. *J Virol* **82**, 2182-2195.



**Taylor, M.P. & Kirkegaard, K. (2007).** Modification of cellular autophagy protein LC3 by poliovirus. *J Virol* **81**, 12543-53.

**Taylor, M.P. & Kirkegaard, K. (2009).** Potential subversion of autophagosomal pathway by picornaviruses. *Autophagy* **4**, 286-289.

**Uchil, P.D. & Satchidanandam, V. (2003).** Architecture of the flaviviral replication complex. Protease, nuclease, and detergents reveal encasement within double-layered membrane compartments. *J Biol Chem* **278**, 24388-24398.

**Wakita, T., Pietschmann, T., Kato, T., Date, T., Miyamoto, M., Zhao, Z., Murthy, K., Habermann, A., Kräusslich, H.G., Mizokami, M., Bartenschlager, R. & Liang, T.J. (2005).** Production of infectious hepatitis C virus in tissue culture from a cloned viral genome. *Nat Med* **11**, 791-796.

**Welsch, S., Miller, S., Romero-Brey, I., Merz, A., Bleck, C.K., Walther, P., Fuller, S.D., Antony, C., Krijnse-Locker, J. & Bartenschlager, R. (2009).** Composition and three-dimensional architecture of the dengue virus replication and assembly sites. *Cell Host Microbe* **5**, 365-75.

**Westaway, E.G., Mackenzie, J.M., Kenney, M.T., Jones, M.K. & Khromykh, A.A. (1997).** Ultrastructure of Kunjin virus-infected cells: colocalization of NS1 and NS3 with double-stranded RNA, and of NS2B with NS3, in virus-induced membrane structures. *J Virol* **71**, 6650-6661.

**Wong, J., Zhang, J., Si, X., Gao, G., Mao, I., McManus, B.M. & Luo H. (2008).** Autophagosome supports coxsackievirus B3 replication in host cells. *J Virol* **82**, 9143-9153.

**Zhong, J., Gastaminza, P., Cheng, G., Kapadia, S., Kato, T., Burton, D.R., Wieland, S.F., Uprichard, S.L., Wakita, T. & Chisari, F.V. (2005).** Robust hepatitis C virus infection in vitro. *Proc Natl Acad Sci USA* **102**, 9294-9299.

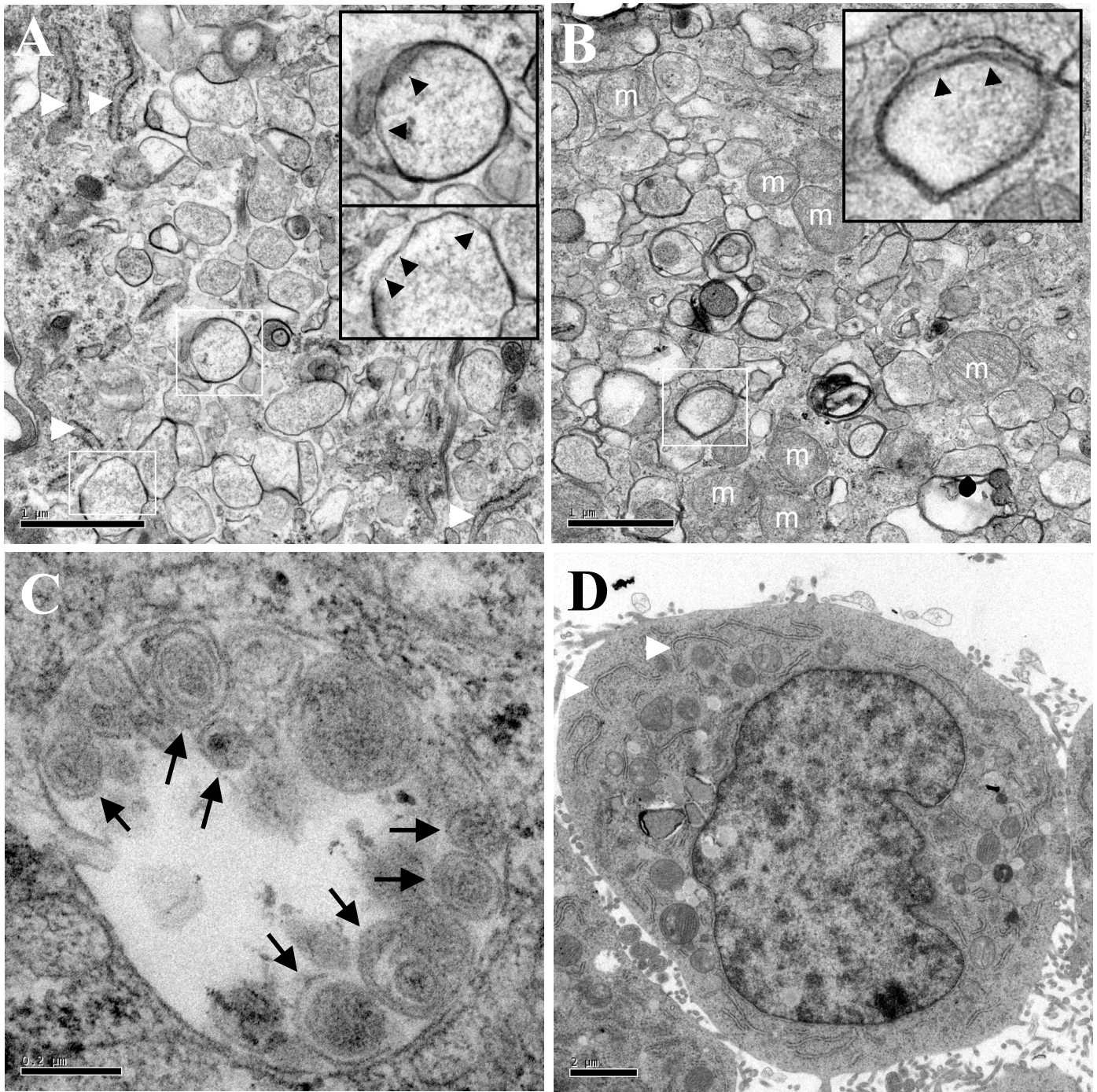
### *Figure legends*

**Fig. 1.** Main ultrastructural changes in Huh7.5-C5 cells harboring a subgenomic replicon of the JFH-1 strain. (A and B): The cells were characterized by the presence throughout the cytoplasm of 200 to 500 nm-wide vesicles with a thick, electron-dense membrane, which were clearly different from the normal lamellar ER membranes (white arrowheads in panel A) and mitochondria (m in panel B). A careful examination of these structures at a higher magnification showed that this thick membrane actually consisted of two closely apposed membranes, as a double membrane could be discerned in some areas (black arrowheads in the vesicle shown in the insets of panels A and B — the enlarged vesicles shown in the insets are indicated by the white square in the corresponding panel). These structures shown in panels A and B were highly specific to Huh7.5-C5 cells, and were rarely found in the Huh7.5 control cells. (C): A less frequent ultrastructural feature of the Huh7.5-C5 cells was the presence of large single-membrane vesicles (up to 800 nm across), containing several circular units (black arrows), 150 to 200 nm-wide, consisting of concentric membranes surrounding a denser core. These structures were never found in the Huh7.5 control cells. (D) Control Huh7.5 cells displayed normal rough ER (white arrowheads). Bars, 1 micrometer (A, B), 0.2 micrometers (C), and 2 micrometers (D).

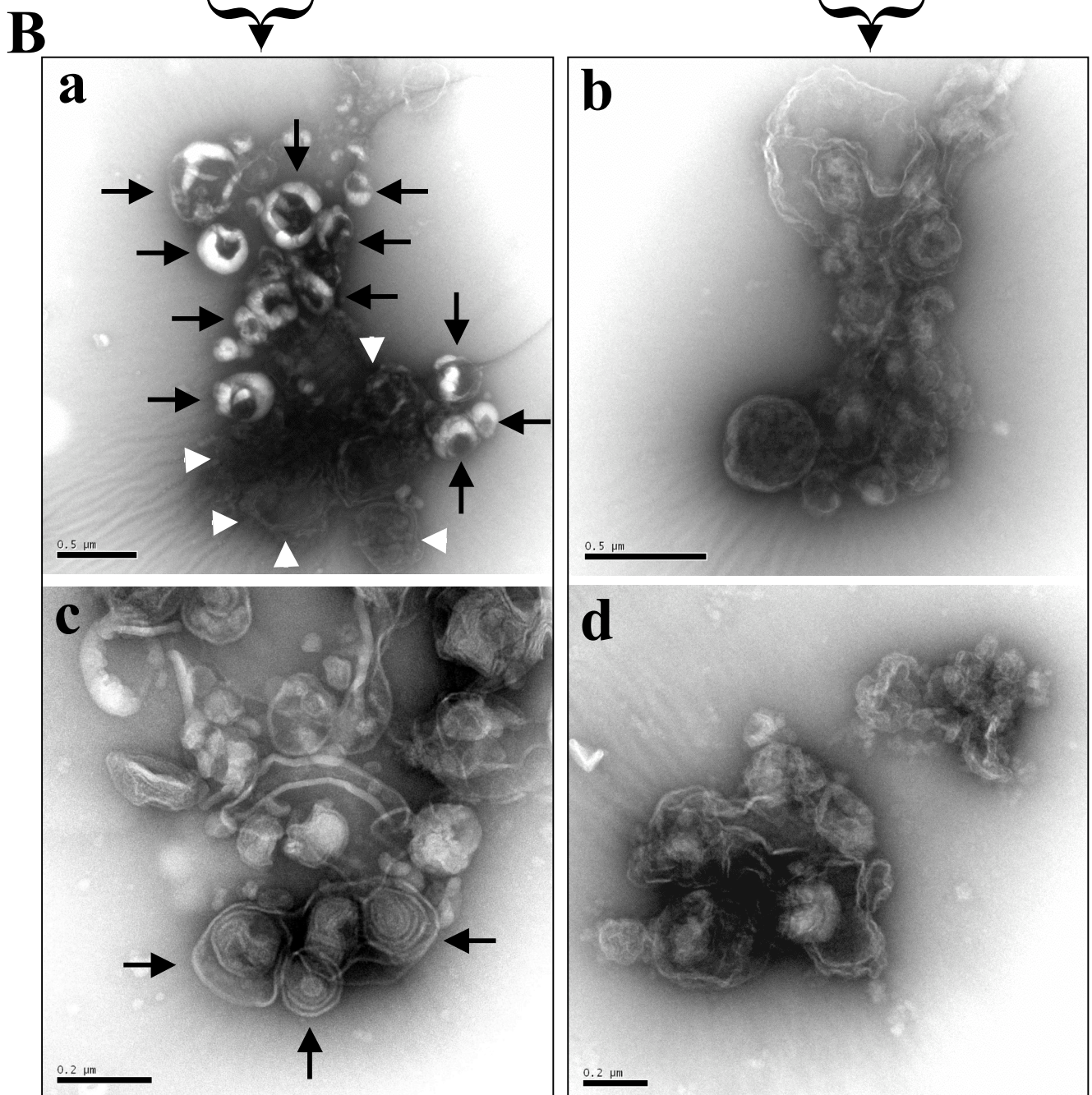
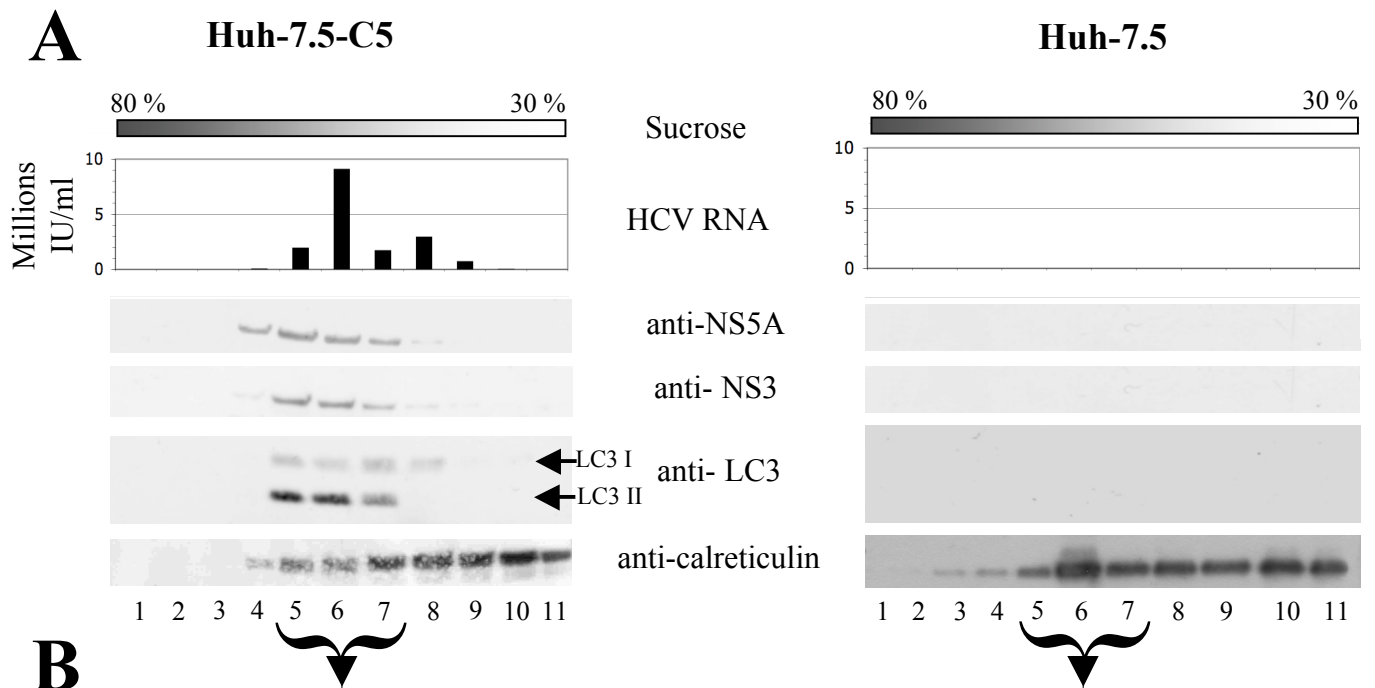
**Fig. 2.** Analysis by real-time PCR, western blotting and negative-staining EM of the Huh7.5-C5 and Huh7.5 cell homogenates separated on a sucrose gradient. (A): HCV RNA, represented here in millions of IU/ml (Abbott m2000<sub>sp</sub>-m2000<sub>rt</sub> real-time PCR assay), peaked in fractions 5 to 8 of the gradient. Membranes of the Huh7.5-C5 cells sedimenting on three of these fractions (5, 6 and 7), corresponding to a density of 1.18 to 1.27 g/cm<sup>3</sup>, were also positive for NS5A and NS3. These fractions also tested positive for the autophagosome marker LC3-II and, to a lesser extent, its precursor, LC3-I. None of these markers was found in the equivalent fractions from the Huh7.5 control cells. Fractions 5 to 11 (1.02 to 1.18 g/cm<sup>3</sup>) tested positive for the ER marker calreticulin, for both Huh7.5-C5 and Huh7.5 cells. (B): Fractions 5 to 7 were pooled for each of the cell lines (Huh7.5-C5 and Huh7.5) and analyzed by EM with negative staining. For both cell types, these fractions contained nonspecific smooth membranes (structures indicated by white arrowheads in B-a; similar structures were found in the control, as shown in B-b and B-d). Fractions from the Huh7.5-C5 cells also contained highly specific structures associated with these smooth membranes (B-a

and B-c). These specific structures included 200 to 500 nm-wide vesicles with a very thick membrane (black arrows in B-a) and 150 to 200 nm-wide circular units containing a core surrounded by concentric membranes (black arrows in B-c). Clusters of these circular structures seemed to be enclosed by a wrapping membrane (B-c). Bars, 0.5 micrometers (B-a and B-b), 0.2 micrometers (B-c and B-d).

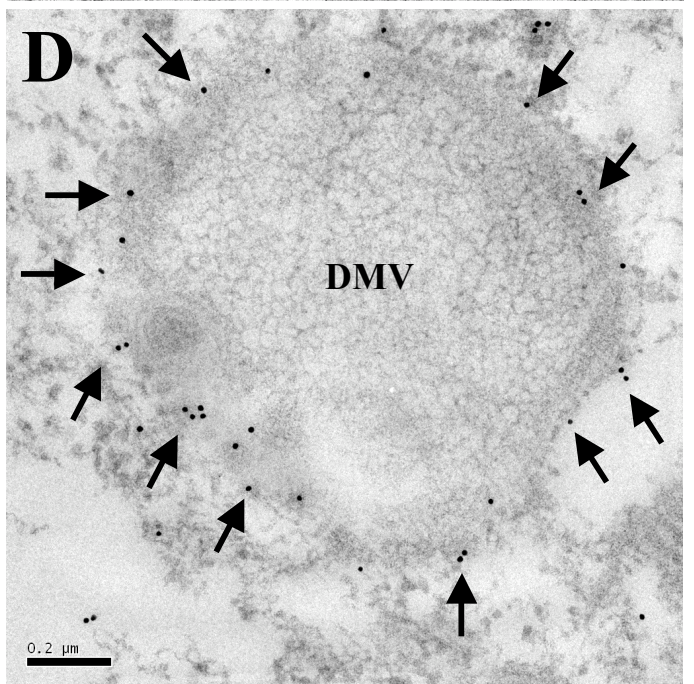
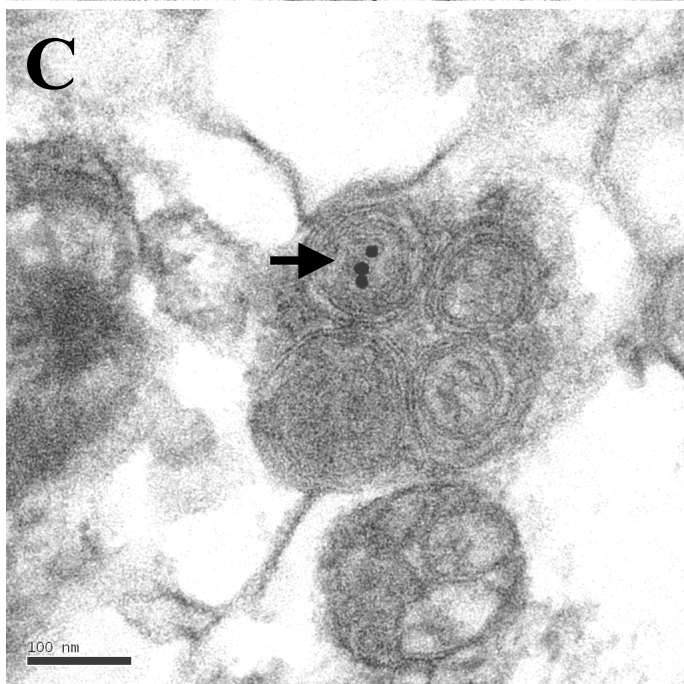
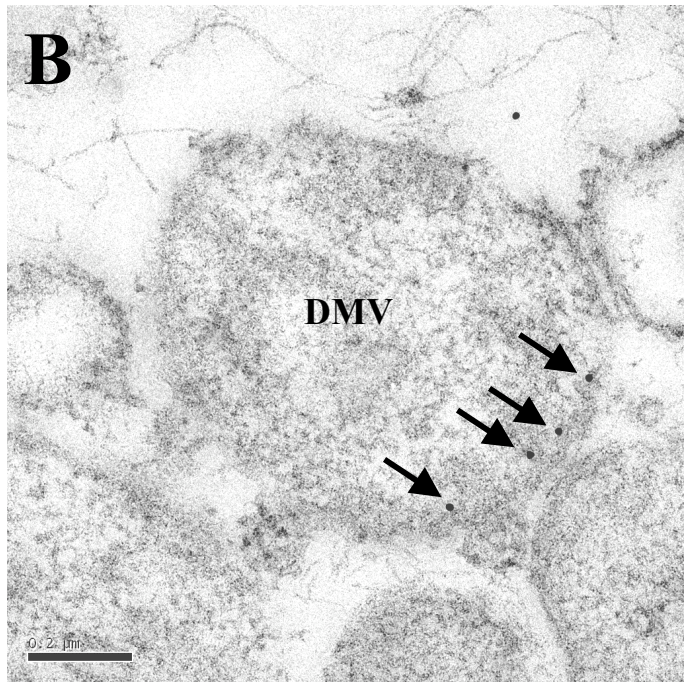
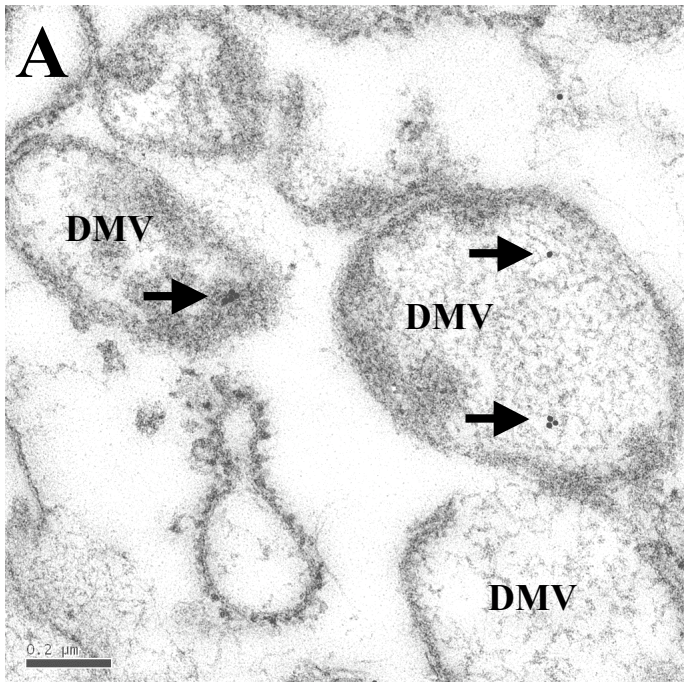
**Fig. 3.** Immuno-EM analysis of ultrathin sections of Huh7.5-C5 cells prepared by cryosubstitution. (A): Immuno-gold labeling with the anti-dsRNA monoclonal antibody was faint but mostly within the DMVs. (B and C): Immunogold labeling with anti-NS5A antibodies was observed at the inner membrane of the DMVs (B) or within the circular units containing concentric membranes (C). (D): In cells transfected with pEGFP-LC3, immunogold labeling with the anti-GFP antibody strongly decorated the surrounding membranes of the DMVs. These observations were specific to Huh7.5-C5 cells, as no immunogold labeling was detected in the Huh7.5 control cells (data not shown). Bars, 0.2 micrometers (A, B and D), 100 nanometers (C).



Ferraris et al, Fig 1



Ferraris et al, Fig 2



Ferraris et al, Fig 3